Kinetic energy of ^{4}He along the $T=6.1$ K isotherm

M. Celli and M. Zoppi
Consiglio Nazionale delle Ricerche, Istituto di Elettronica Quantistica, Via Panciatichi 56/30, I-50127 Firenze, Italy

J. Mayers
Rutherford Appleton Laboratory, ISIS Neutron Facility, Chilton, Didcot, OX11 0QX, United Kingdom

(Received 2 September 1997; revised manuscript received 23 January 1998)

We report the results of a neutron Compton scattering experiment on ^{4}He, on the $T=6.1$ K isotherm, in a wide density range extending from the low-density gas phase to the compressed solid. These experiments give access to the atomic momentum distribution and we have derived the average kinetic energy. This is a function of the density, due to the increasing effect of interactions in the quantum fluid, and equals the classical value $\frac{3}{2}k_BT$ only in the zero-density limit. The data allow us to give a coherent picture of the evolution of the kinetic energy of ^{4}He, on the $T=6.1$ K isotherm, up to the compressed solid phase ($p_{max}=539$ bars) where the measured value of the kinetic energy is ~ 5 times larger than the classical value. The data in the fluid phase are well described by a power law in the density with exponent 2.46. We confirm that the kinetic energy data display a change of behavior across the freezing transition, with the solid data *lower* than the extrapolation of the fluid data. [S0163-1829(98)02922-1]

I. INTRODUCTION

Deep inelastic neutron scattering is an experimental technique that can be used to probe *directly* the momentum distribution of atoms in condensed matter.[1,2] In fact, if very-high-energy neutrons are used as a probe and the momentum transfer becomes sufficiently high that the interference effects due to the correlations between neighbors become negligible, then the *incoherent scattering approximation* holds and the process simply becomes a sum of single-atom scattering events where the neutron loses some of its energy that is transferred to the nucleus as a recoil energy.[3] This energy is related to the momentum transfer $\hbar q$ by the simple relation $\hbar\omega=(\hbar q)^2/2m$, where m is the mass of the recoiling atom.[3] Since the energy of the neutrons is much larger than any energy involved in the atomic system (5 eV corresponds to 58 000 K), the process is not expected to be influenced by the local environment of the nuclei.[4] For this reason, the phenomenon is also referred to as neutron Compton scattering (NCS).[5] By means of NCS we have direct access to the momentum distribution of particles, which is the space Fourier transform of the single-particle density matrix. A comprehensive review of the field can be found in Ref. 6.

For monatomic classical systems (e.g., liquid and solid argon, krypton, and xenon, at not too low temperature) the momentum distribution $n(\mathbf{p})$ is generated by the Maxwell-Boltzmann distribution, i.e., it has a Gaussian shape whose width is simply given by the mean kinetic energy $E_k=\frac{3}{2}k_BT$.[7] As the atomic mass decreases, like, for example, in neon, quantum effects emerge and the kinetic energy increases with respect to the classical expectation. The shape of the momentum distribution, however, is still assumed Gaussian.[8–10]

The case of helium is particular. Due to the combined effects of the small atomic mass and the low temperature of the condensed phases, quantum effects can no longer be considered a small correction to an essentially classical behavior and the discrepancy between the measured kinetic energy and its classical counterpart becomes sizable. Again, the shape of the momentum distribution appears to be Gaussian.[11] However, more recent experiments on liquid ^{4}He were analyzed by assuming for the shape of the momentum distribution a sum of two Gaussians with the same peak position.[12] At any rate, the kinetic energy, which is proportional to the second moment of the scattering function, shows a definite breakdown of the classical picture.

NCS experiments on helium were carried out with the aim of measuring the atomic kinetic energy in a condensed quantum system. At first sight, it appears that this quantity does not depend on the microscopic structure but only on the density. In fact, experiments carried out in a hcp solid at 1.60 K and 0.96 K,[1] in a *bcc* solid at 1.70 K,[13] and in the liquid phase at 4.0 K, all at the same density of 27.7 nm^{-3}, resulted in a common value for the kinetic energy $E_k=19.5$ K.[14] In contrast, the theoretical values obtained by using the Green function Monte Carlo method were 20.7 K and 21.8 K for the liquid and the solid, respectively.[15] In a more recent experiment,[12] the average kinetic energy of liquid ^{4}He was measured on the 4.25-K isotherm between the liquid-vapor saturation line ($n=18.8$ nm^{-3}) up to a pressure of 103.4 bars, corresponding to the density $n=30.1$ nm^{-3}. The average kinetic energy shows a clear dependence on the density. A quadratic fit to the data seems to describe quite well the density behavior, even though no theoretical justification exists for this function. The data were also compared with the path integral Monte Carlo (PIMC) simulations of Ceperley and Pollock[16] and satisfactory agreement was found. However, it appears that this agreement becomes of lesser quality at the highest densities.

A similar parabolic law of the kinetic energy as a function of density (at constant temperature) was also found to fit the PIMC simulations of solid para-hydrogen.[17] Also in this case, the agreement between the simulation data and the experiment[18] is satisfactory. However, the extension of the

simulations to the liquid phase reveals that either the observed parabolic law breaks down at the lowest densities or its coefficients may depend on the phase of the system. In fact, the simulation data suggest that, in the liquid phase, the kinetic energy has a density behavior different from that in the solid.[19] Whether this is a signature of some kind of dependence upon the microscopic structure of the system or just a mere failure of the simple heuristic parabolic law is not known.

For helium, no such extended range of experimental data was available from a single experiment. In fact, an extensive measurement of the kinetic energy as a function of density was reported by Herwig *et al.*,[12] which only covers a portion of the liquid range (up to about 100 bars) on the 4.25-K isotherm. More experimental data were reported later by Blasdell *et al.*,[20] who extended the measurements to the solid phase. However, the authors did not consider the high-density data free from systematic uncertainties.

For these reasons, with the aim of obtaining from a single experiment information covering a wide density range and eventually crossing the melting transition, we carried out a NCS experiment on helium at constant temperature $T=4.35$ K.[21] The pressure interval was between 35 and 500 bars. This ample pressure range allowed us to cross the melting transition of helium, thus extending the experimental investigation on both phases. The data in the liquid phase turned out consistently with the previous experiments. In addition, we found a discontinuity in the density behavior of the kinetic energy across the melting transition with the values of the kinetic energy, measured in the solid phase, *lower* than the extrapolation of the liquid phase data.[21] Unfortunately, the densities that were assigned to the solid phase data in this experiment were found to be erroneous in a following check, due to a likely difference between the internal and external pressure of the sample.

We discovered the mistake after performing a *second* experiment, carried out at a slightly different temperature ($T=6.1$ K), in which we had taken advantage of the possibility offered by the resonance spectrometer eVS of measuring, at the same time, the momentum distribution *and* the diffraction pattern of the sample.[22] This experiment was characterized by an improved accuracy in the density determination of the solid phase, measured from the position of the Bragg peaks in the neutron diffraction spectra of helium. A short account of the second experiment has been already published and we recall here the main results that were reported in Fig. 2 of Ref. 22. Even though we had found a confirmation of the previous qualitative behavior, i.e., that the solid state kinetic energy data were *lower* than the extrapolation of the fluid phase data, we were not fully satisfied with these results. We note that there is a lack of experimental data in the intermediate-density range and that, in practice, the choice between the different functional forms was mainly based on an interpolation of experimental points that were taken by a third party.[23] As any experiment is affected by *its* systematic errors, though small, this could have represented a weak point in our conclusions.

For this reason, we have carried out a *third* experiment, using essentially the same experimental setup as the second, with the aim of covering the intermediate-density region. In this way we were able to build up a very coherent picture of the density behavior of the kinetic energy of ^{4}He on the $T=6.1$ K isotherm. The main advantage of operating at a temperature slightly above the critical value is that the experiment in the fluid phase could be carried out in the whole density range between the ideal gas limit and the freezing transition. Here we will give a full description of the whole experiments at $T=6.1$ K and we will describe the details of the data analysis. Finally, we will show that our finding for the kinetic energy in the solid phase is actually *lower* than the extrapolation of the liquid phase data.

II. DESCRIPTION OF EXPERIMENT

The experiments were carried out on the eVS spectrometer of the pulsed neutron source ISIS. This is an inverse geometry inelastic spectrometer that uses a resonance absorption filter (a gold foil) as an energy analyzer in the secondary neutron path. A detailed description of the instrument and its calibration procedure is reported in Ref. 24.

In order to evenly cover the whole density range of helium between 0 and 539 bars at $T=6.1$ K, the experiment was completed in two steps. The same aluminum alloy (7075) was used to manufacture two sample containers. In the first experimental run, we used a pressure vessel able to hold the maximum planned pressure of 500 bars with a suitable security factor. In the second, to compensate for the decrease in the recorded signal at lower densities, a thinner wall and a larger sample volume were designed. In this case, the maximum allowed pressure was only of 50 bars.

In either case, the sample cell was adapted into a liquid helium cryostat. This was connected to the external gas handling system by means of a stainless steel tube of 1/16 in. outside diameter. The filling tube was wrapped with an electric heater in order to avoid blockage. The upper and lower body of the cell were in good thermal contact with copper blocks, which were independently temperature controlled and stabilized. The temperature stability during the whole experiment was found to be better than 0.02 K. The temperature difference between the top and bottom copper blocks was always less than 0.1 K. We assume, for our helium sample, an average temperature $T=6.1\pm0.1$ K.

For the high-pressure experiment, the scattering cell was initially filled with gaseous helium ($p\simeq150$ bars) and then cooled down to the desired temperature. Once the system was in thermal equilibrium, we started the data collection for two different pressures (171 and 220 bars) in the fluid phase. The sample was then pressurized, up to a maximum pressure of 539 bars, to collect the data from the solid phase (nine thermodynamic points). Each time we carried out a pressure change, the heater on the inlet pipe was temporarily turned on and we observed a rise in the temperature of the cell. The system was then stabilized back to the equilibrium temperature ($T=6.1$ K) and the following data acquisition run was started. Finally, we ended this experimental cycle with four more runs in the fluid phase. The details of this experiment are reported in Table I and a brief account of the results has been reported in Ref. 22.

For the low-pressure experiment, we started with the highest pressure of 34.8 bars, followed by four lower pressure points. In this case, no particular problem in temperature stabilization was observed. The details of this experimental

TABLE I. Experimental details of the first experimental cycle: dense fluid and solid in the high-pressure container. The pressure was measured on an external gauge connected to the gas handling system. The temperature of the sample was $T=6.1\pm0.1$ K. The densities in the fluid phase were calculated using Ref. 25. For the solid phase we used the experimental determination of the lattice parameters by means of the Bragg peaks. IPC stands for integrated proton current and is a measure of the duration of the run.

p (bars)	n (nm^{-3})	IPC (μAh)	Phase
539±5	44.4±0.1	1979	solid
502±5	43.7±0.1	997	solid
491±5	43.6±0.1	2180	solid
457±5	42.7±0.1	2190	solid
394±5	42.2±0.2	2152	solid
347±5	41.2±0.1	887	solid
335±5	40.8±0.1	1011	solid
314±5	40.7±0.1	1071	solid
264±3	39.5±0.2	2044	solid
220±3	35.2±0.2	2475	fluid
199±3	34.5±0.2	1181	fluid
171±3	33.2±0.2	2993	fluid
107±3	30.7±0.2	1788	fluid
73±3	28.5±0.2	2117	fluid
2.9±0.5	6.0±2.0	2030	fluid

cycle are reported in Table II.

While the determination of the sample density in the fluid phase was straightforward,[25] the same procedure appeared to give erroneous results in the solid phase. As explained above, we had observed that heating the inlet pipe of the cell, in order to release part of the pressure, the sample slightly changed its thermal status, essentially because of the low heat capacity at this low temperature. During the subsequent relaxation towards the thermal equilibrium, we could observe the evolution of the sample from the changes in temperature and in pressure. However, after turning off the heater, we could not make sure that the sample inside the cell experienced the same pressure that we could read on the (external) gauge, because of the freezing of helium in the inlet pipe. We were able to overtake this difficulty when we realized that we could extend the time range of the time of flight (TOF) spectra up to a point including the Bragg peaks

TABLE II. Experimental details of the second experimental cycle: fluid helium in the low-pressure container. The pressure was measured on an external gauge connected to the gas handling system. The temperature of the sample was $T=6.1\pm0.1$ K. The densities in the fluid phase were calculated using Ref. 25. IPC stands for integrated proton current and is a measure of the duration of the run.

p (bars)	n (nm^{-3})	IPC (μAh)	Phase
34.85±0.05	25.04±0.01	1730	fluid
23.20±0.05	23.24±0.01	2304	fluid
11.70±0.05	20.19±0.02	2131	fluid
5.81±0.05	16.10±0.03	3294	fluid
3.84±0.05	10.18±0.03	4296	fluid

of solid helium. This information could be used for density calibration. The solid phase densities, reported in Table I, are obtained by this procedure.

In both experimental cycles, we used four detector banks, each made of eight scintillator counters, placed in almost backscattering geometry. In the first one, the measured angular interval was in the range $92.25°-147.80°$. Given the measured value of the energy resonance of the gold foil, the value of the momentum transfer, evaluated on the recoil peak of helium, is between 81.6 and 122.3 $Å^{-1}$. In the second, the interval of scattering angles was between 83.5° and 148.7° and the corresponding momentum transfer interval turned out to be between 73.6 and 122.6 $Å^{-1}$. The measured resonance energy of the gold foil turned out to be 4.909 eV with a half-width of 127 meV.

There are five independent contributions to the instrument resolution function. Four are of geometrical origin and derive from the uncertainties in the primary path L_0, the secondary path L_1, the neutron time of flight τ, and the finite size of the collection solid angle. The fifth is determined by the width of the resonance absorption line of the analyzing filter. For a gold foil, the overall shape of the absorption line is a Lorentzian function.[26] The geometrical contributions, instead, are well represented by Gaussian distributions and are evaluated by means of a Monte Carlo simulation routine. Therefore, the overall resolution function turns out to be a Voigt profile. In the present experimental configuration, the standard deviation of the angular contribution (Gaussian) is 3 times smaller than the gold foil term. The other geometrical contributions are even smaller. Thus we end up with an intrinsic instrumental resolution function whose half-width at half maximum is of the order of 150 meV.

The observed spectra are of similar quality in both experiments, with an improved signal-to-background ratio in the low-density experiment, where a thinner container was used. Typical TOF spectra were shown in Fig. 1 of Ref. 22. We observe that the container contribution to the TOF spectra can be easily removed, as it affects a different spectral region. Moreover, the contributions from multiple scattering processes were evaluated by means of a Monte Carlo routine and were found to be very small with respect to the primary scattering.

III. DATA ANALYSIS AND RESULTS

Given the high values of the momentum transfer that are probed by the present experiment, we could safely operate within the impulse approximation (IA) framework.[2] The validity of such a formalism was successfully tested by Herwig *et al.*[12] in a previous experiment on liquid helium where the momentum transfer was limited to ~ 23 $Å^{-1}$. This is also substantiated, for normal liquid helium above the λ transition, by Silver's theoretical work.[27] However, below the superfluid transition, or for lower values of the momentum transfer, the broadening induced by final-state effects should be taken into account.[28,27]

Within the range of validity of the IA, a scaling variable y can be defined as[2]

$$y=\left(\frac{m}{\hbar q}\right)\left(\omega-\frac{\hbar q^2}{2m}\right), \tag{1}$$

where $\hbar\mathbf{q}$ and $\hbar\omega$ are the momentum and energy transfer, respectively, and m is the mass of the target nucleus. With this definition y has the same dimension as q. Thus the scattering function can be expressed by means of the scaling variable and becomes

$$S(\mathbf{q},\omega)=\frac{m}{\hbar q}J(\hat{\mathbf{q}},y), \tag{2}$$

where $J(\hat{\mathbf{q}},y)$, usually referred to as the *Compton profile*, is defined as

$$J(\hat{\mathbf{q}},y)=\int n(\mathbf{p})\,\delta\left[\left(\frac{\mathbf{p}\cdot\mathbf{q}}{q}\right)-y\right]d\mathbf{p} \tag{3}$$

and $\hat{\mathbf{q}}$ represents the unit vector of $\mathbf{q}$, while $\hbar\mathbf{p}=m\mathbf{v}$ is the momentum of the target atom.

As we have seen in the Sec. II, the width of the instrumental resolution function is of the order of 150 meV. That is considerably larger than the width of the intrinsic momentum distribution. For example, at the smallest scattering angle (lowest q) the intrinsic width ranges between $\sim$55 and $\sim$80 meV (lowest and highest density of the present experiment), while at the highest q value these values become $\sim$95 and $\sim$135 meV, respectively. As a consequence, in the present experimental configuration, it ends up being very difficult to make evident in the Compton profile deviations from a pure Gaussian shape, as it was suggested by the PIMC simulations by Ceperley and Pollock.[16] At any rate, we have attempted such a procedure and we found that including a second Gaussian component in the fitting function, without imposing arbitrary constraints on the parameters, affects the stability of the fitting procedure. Therefore, also to maintain a coherent picture with the previous experiment, we have assumed that the momentum distribution $n(\mathbf{p})$ can be fitted with a pure Gaussian profile.

Returning to Eq. (3), we obtain that the same Gaussian profile is characteristic of the function $J(\hat{\mathbf{q}},y)$. In the fluid phase, the sample is isotropic and the dependence on the unit vector $\hat{\mathbf{q}}$ becomes irrelevant. However, also in the solid phase, no evidence of anisotropic behavior has been observed by NCS.[29] Therefore, the Compton profile becomes simply $J(y)$ for both the fluid and the solid phase and its functional form reduces to

$$J(y)=(2\pi\sigma^2)^{-1/2}\exp\left(-\frac{y^2}{2\sigma^2}\right), \tag{4}$$

where σ is given by the average atomic kinetic energy

$$\langle E_k\rangle=\frac{3}{2}\frac{(\hbar\sigma)^2}{m}. \tag{5}$$

Due to the different scattering angle of the various detectors, each experimental spectrum was analyzed separately. After subtracting the container contribution, the width of the experimental Compton profile was obtained, according to Eq. (4), using a convolution between a pure Gaussian shape and the instrumental resolution function. Then, for each spectrum, the value for the atomic average kinetic energy was derived using Eq. (5). In this way, the final average and error on E_k was determined by the value and the variance of the 32 independent data obtained by the various spectra. We point out, once again, that exactly the same procedure was applied to both the fluid and the solid phase data. Therefore, should any systematic error affect the experimental data, this would influence equally all the measured points.

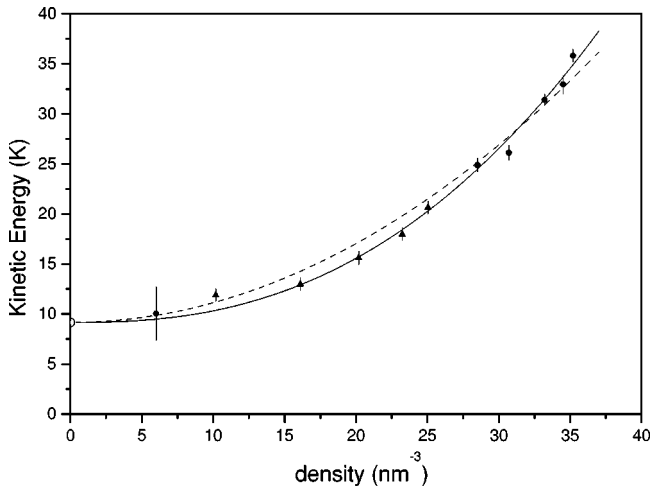

FIG. 1. Mean experimental kinetic energy of fluid helium as a function of density at constant temperature $T=6.1$ K. The triangles represent the present data, the full circles refer to the previous experiment, and the open circle at $n=0$ is the classical value that is obtained from the temperature of the sample. The error bars are obtained by averaging over the 32 independent detector spectra. The full line is the best fit using a power law with exponent 2.46 (see the text). The reduced χ^2 for this fit turns out to be 1.56. The dashed line is a parabolic fit. In this case the reduced χ^2 is 4.02.

In Fig. 1 we report the density evolution of the kinetic energy of helium in the fluid phase. The present data are represented by the triangles, while the full circles represent the results of the first experimental cycle. The point at $n=0$ is the classical value that is obtained from the temperature of the sample. In this isotropic phase, the interactions give a rather large contribution to the kinetic energy that increases by more than a factor of 3 from the low- to the high-density region. First the data were fitted using a parabolic law in addition to the classical term $\frac{3}{2}k_BT$. This is represented by the dashed line in Fig. 1. The agreement is far from satisfactory. In fact, the reduced χ^2 for this fit turns out to be rather large ($\chi^2_{red}=4.02$). Then we attempted a nonlinear fit using a power law. The result is a density dependence $E_k=\frac{3}{2}k_BT+Bn^{2.46}$ and is represented by the full line in the graph. This function appears to be much closer to the experimental results, as is confirmed by the reduced χ^2 that, for this fit, turns out to be much lower and is $\chi^2_{red}=1.56$. Of course we have no theoretical justification for either function and we base our choice for the power law only on the value of the reduced χ^2.

In Fig. 2 we report the kinetic energy of helium in an extended density range on the $T=6.1$ K isotherm. The freezing pressure at this temperature is 258 bars, corresponding to a liquid density of 36.3 nm^{-3}. The data beyond this point belong to the solid phase. As it appears from the figure, the kinetic energy of solid helium is lower than the extrapolation that is obtained by extending the fitting function of the fluid phase data (power law).

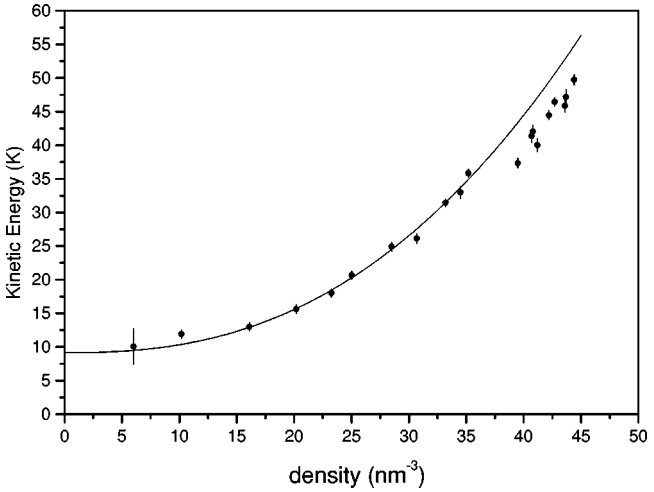

FIG. 2. Mean experimental kinetic energy of fluid and solid helium as a function of density at constant temperature $T=6.1$ K (full circles with error bars now refer to the two experiments mentioned in the text). The data beyond 36.3 nm^{-3} belong to the solid phase. The full line is the best fit (power law) of the fluid phase data that has been extrapolated to higher densities.

IV. CONCLUSIONS

We have measured the kinetic energy of fluid and solid helium on the isotherm $T=6.1$ K. The pressure range was extended up to 539 bars and the data points cover a wide density range, crossing the gap between the fluid and the solid phase. As the critical temperature of helium is $T_c=5.2$ K, there is no gap in the data at low density. Quantum effects on the kinetic energy are relevant and result in a rather strong density dependence. The measure at the highest density is almost a factor of 5 larger than the classical low-density value.

The experimental data for $E_k(n)$, in the fluid phase, have been fitted using a power law of exponent 2.46. This value improves a previous determination (exponent 2.7) that was based on a smaller set of data points.[22] An attempt to use a parabolic fit to the data turned out to be of much lesser quality (cf. Fig. 1). It is worthwhile to point out that the present data are the combined result of two independent experiments, with the second experiment carried out more than one year after the first. The two experiments are in excellent agreement. Moreover, the present experimental data are in rather good agreement with previous results that were carried out at lower temperature (below the critical point), as it is testified by Fig. 3 of Ref. 22.

Extending the fitting function to higher density, so as to include the solid state data range, results in a discrepancy with the measured values. The difference is not very large but is significant (cf. Fig. 2). The solid state kinetic energy data turn out to be *lower* than the extrapolation. It is interesting to note that the kinetic energy behavior, as a function of density, resembles that of the pressure, with a gap crossing the freezing transition. This is not unreasonable, as the kinetic energy is one of the two contributions (the second being the virial contribution) to the value of the pressure.

A lower value for the kinetic energy of the solid, with respect to the extrapolation of the fluid phase, is also consistent with the physical intuition. In fact, a phase transition is expected when, keeping constant the two independent thermodynamic variables, density and temperature, the second phase is characterized by a lower value of the internal energy. If we assume for a moment that the equipartition theorem applies, lowering the kinetic energy is equivalent to lowering the total energy. Therefore, the observed phenomenon is exactly what one should expect for a phase transition.

Finally, the present observations allow us to draw some considerations. Let us assume, for example, two equivalent configurations (same density and temperature), one in an ordered crystal phase and the other in a disordered fluid phase. A lower kinetic energy in the ordered phase and the application of the Heisenberg uncertainty principle result in a larger volume that each atom can use, in the crystal phase, to spread its wave function. As a consequence, if we think of each particle as confined by the cage of its neighbors, it is the lack of fixed lattice positions that makes smaller, on the average, the volume available for an atom in the disordered phase, with respect to the corresponding volume that is available in the ordered crystal phase. It would be interesting to know how this is related to the differences in the density of states of the two phases.

ACKNOWLEDGMENT

The technical assistance of the ISIS Instrument Division of RAL is gratefully acknowledged.

[1] R. O. Hilleke, P. Chaddah, R. O. Simmons, D. L. Price, and S. K. Sinha, Phys. Rev. Lett. **52**, 847 (1984).
[2] V. F. Sears, Phys. Rev. B **30**, 44 (1984).
[3] S. W. Lovesey, *Theory of Neutron Scattering from Condensed Matter* (Oxford University Press, Oxford, 1987).
[4] It should be pointed out that the neutron energies involved in these experiments are smaller than the first electronic transition in helium ($\simeq$19.8 eV) and, therefore, during a NCS experiment on helium, the atoms retain their electronic distribution almost undisturbed.
[5] G. I. Watson, J. Phys.: Condens. Matter **8**, 5955 (1996).
[6] *Momentum Distribution*, edited by R. N. Silver and P. E. Sokol (Plenum, New York, 1989).
[7] D. A. Peek and R. O. Simmons, J. Chem. Phys. **94**, 3169 (1991).
[8] D. A. Peek, M. C. Schmidt, I. Fujita, and R. O. Simmons, Phys. Rev. B **45**, 9671 (1992).
[9] D. A. Peek, I. Fujita, M. C. Schmidt, and R. O. Simmons, Phys. Rev. B **45**, 9680 (1992).
[10] D. N. Timms, A. C. Evans, M. Boninsegni, D. M. Ceperley, J. Mayers, and R. O. Simmons, J. Phys.: Condens. Matter **8**, 6665 (1996).
[11] A. D. B. Woods and V. F. Sears, Phys. Rev. Lett. **39**, 415 (1977).
[12] K. W. Herwig, P. E. Sokol, T. R. Sosnick, W. M. Snow, and R. C. Blasdell, Phys. Rev. B **41**, 103 (1990).
[13] P. E. Sokol, R. O. Simmons, D. L. Price, and R. O. Hilleke, Physica B&C **126**, 1213 (1984).

[14] R. O. Simmons and P. E. Sokol, Physica B&C **136**, 156 (1986).
[15] P. A. Whitlock, D. M. Ceperley, G. V. Chester, and M. H. Kalos, Phys. Rev. B **19**, 5598 (1979).
[16] D. M. Ceperley and E. L. Pollock, Phys. Rev. Lett. **56**, 351 (1986).
[17] M. Zoppi and M. Neumann, Phys. Rev. B **43**, 10 242 (1991).
[18] K. W. Herwig, J. L. Gavilano, M. C. Schmidt, and R. O. Simmons, Phys. Rev. B **41**, 96 (1990).
[19] M. Zoppi and M. Neumann, Physica B **180&181**, 825 (1992).
[20] R. C. Blasdell, D. M. Ceperley, and R. O. Simmons, Z. Naturforsch. Teil A **48A**, 433 (1993).
[21] U. Bafile, M. Zoppi, F. Barocchi, R. Magli, and J. Mayers, Phys. Rev. Lett. **75**, 1957 (1995).
[22] U. Bafile, M. Zoppi, F. Barocchi, R. Magli, and J. Mayers, Phys. Rev. B **54**, 11 969 (1996).
[23] C. Andreani, A. Filabozzi, M. Nardone, F. P. Ricci, and J. Mayers, Phys. Rev. B **50**, 12 744 (1994).
[24] J. Mayers and A. C. Evans, Rutherford Appleton Laboratory Report No. RAL-91-048, 1991 (unpublished).
[25] R. McCarty, J. Phys. Chem. Ref. Data **2**, 923 (1973).
[26] P. A. Seeger, A. D. Taylor, and R. M. Brugger, Nucl. Instrum. Methods Phys. Res. A **240**, 98 (1985).
[27] R. N. Silver, Phys. Rev. B **39**, 4022 (1989).
[28] T. R. Sosnick, W. M. Snow, and P. E. Sokol, Phys. Rev. B **41**, 11 185 (1990).
[29] A. C. Evans (private communication).